Inorg. Chem. **2005**, *44*, 2150–2158

Oxidations of NADH Analogues by *cis*-$[Ru^{IV}(bpy)_2(py)(O)]^{2+}$ Occur by Hydrogen-Atom Transfer Rather than by Hydride Transfer

Takashi Matsuo[†] **and James M. Mayer***

Department of Chemistry, University of Washington, Campus Box 351700, Seattle, Washington 98195-1700

Received December 27, 2004

Oxidations of the NADH analogues 10-methyl-9,10-dihydroacridine ($AcrH_2$) and *N*-benzyl 1,4-dihydronicotinamide (BNAH) by *cis*-$[Ru^{IV}(bpy)_2(py)(O)]^{2+}$ (**$Ru^{IV}O^{2+}$**) have been studied to probe the preferences for hydrogen-atom transfer vs hydride transfer mechanisms for the C–H bond oxidation. ^{1}H NMR spectra of completed reactions of $AcrH_2$ and **$Ru^{IV}O^{2+}$**, after more than ~20 min, reveal the predominant products to be 10-methylacridone (AcrO) and *cis*-$[Ru^{II}(bpy)_2(py)(MeCN)]^{2+}$. Over the first few seconds of the reaction, however, as monitored by stopped-flow optical spectroscopy, the 10-methylacridinium cation ($AcrH^+$) is observed. $AcrH^+$ is the product of net hydride removal from $AcrH_2$, but hydride transfer cannot be the dominant pathway because $AcrH^+$ is formed in only 40–50% yield and its subsequent oxidation to AcrO is relatively slow. Kinetic studies show that the reaction is first order in both **$Ru^{IV}O^{2+}$** and $AcrH_2$, with $k = (5.7 \pm 0.3) \times 10^3$ M^{-1} s^{-1} at 25 °C, $\Delta H^{\ddagger} = 5.3 \pm 0.3$ kcal mol^{-1} and $\Delta S^{\ddagger} = -23 \pm 1$ cal mol^{-1} K^{-1}. A large kinetic isotope effect is observed, $k_{AcrH_2}/k_{AcrD_2} = 12 \pm 1$. The kinetics of this reaction are significantly affected by O_2. The rate constants for the oxidations of $AcrH_2$ and BNAH correlate well with those for a series of hydrocarbon C–H bond oxidations by **$Ru^{IV}O^{2+}$**. The data indicate a mechanism of initial hydrogen-atom abstraction. The acridinyl radical, $AcrH^{\bullet}$, then rapidly reacts by electron transfer (to give $AcrH^+$) or by C–O bond formation (leading to AcrO). Thermochemical analyses show that $H^{\bullet}$ and H^- transfer from $AcrH_2$ to **$Ru^{IV}O^{2+}$** are comparably exoergic: $\Delta G^{\circ} = -10 \pm 2$ kcal mol^{-1} ($H^{\bullet}$) and -6 ± 5 kcal mol^{-1} (H^-). That a hydrogen-atom transfer is preferred kinetically suggests that this mechanism has an equal or lower intrinsic barrier than a hydride transfer pathway.

Introduction

Oxidations of C−H bonds are of fundamental importance, from biochemical to industrial processes.[1] Metal−oxo compounds are often implicated as the key species in these reactions. The key initial mechanistic step in C−H bond oxidations is often electron (e^-) transfer, hydrogen-atom ($H^{\bullet}$) transfer, or hydride (H^-) transfer.[2−9] However, there is little understanding as to why one path would be preferred over another. To probe these issues, we describe here studies of *cis*-$[Ru^{IV}(bpy)_2(py)(O)]^{2+}$ [**$Ru^{IV}O^{2+}$**, **Ru** ≡ $Ru(bpy)_2(py)$] oxidizing the common NADH analogues 10-methyl-9,10-

* To whom correspondence should be addressed. E-mail: mayer@chem.washington.edu.

[†] Current address: Department of Chemistry and Biochemistry, Graduate School of Engineering, Kyushu University, Fukuoka 812-8581, Japan.

(1) (a) Stewart, R. *Oxidation Mechanisms*; Benjamin: New York, 1964. (b) *Organic Synthesis by Oxidation with Metal Compounds*; Mujs, W. J., de Jonge, C. R. H. I., Eds.; Plenum: New York. 1986. (c) Olah, G. A. Molnár, Á. *Hydrocarbon Chemistry*; Wiley: New York, 1995. (d) *Chem. Rev.* **1996**, *96* (7), 2237−3042. (e) *Biomimetic Oxidations Catalyzed by Transition Metal Complexes*; Meunier, B., Ed.; Imperial College Press: London 2000.

(2) Mayer, J. M. *Acc. Chem. Res.* **1998**, *31*, 441−450.

(3) Carrell, T. G.; Bourles, E.; Lin, M.; Dismukes, G. C. *Inorg. Chem.* **2003**, *42*, 2849−2858.

(4) Wiberg, K. B.; Freeman, F. *J. Org. Chem.* **2000**, *65*, 573−576.

(5) (a) Roth, J. P.; Mayer, J. M. *Inorg. Chem.* **1999**, *38*, 2760−2761. (b) Larsen, A. S.; Wang, K.; Lockwood, M. A.; Rice, G. L.; Won, T.-J.; Lovell, S.; Sadílek, M.; Turecek, F.; Mayer, J. M. *J. Am. Chem. Soc.* **2002**, *124*, 10112−10123. (c) Roth, J. P.; Yoder, J. C.; Won, T.-J.; Mayer, J. M. *Science* **2001**, *294*, 2524−2526. (d) Goldsmith, C. R.; Jonas, R. T.; Stack, T. D. P. *J. Am. Chem. Soc.* **2002**, *124*, 83−96. (e) Lykakis, I. N.; Tanielian, C.; Orfanopoulos, M. *Org. Lett.* **2003**, *5*, 2875−2878.

(6) Meyer, T. J.; Huynh, M. H. V. *Inorg. Chem.* **2003**, *42*, 8140−8160 and references therein.

(7) Che. C−M.; Yam, V. W. W. *Adv. Transition Met. Coord. Chem.* **1996**, *1*, 209−237.

(8) (a) Bryant, J. R.; Mayer, J. M. *J. Am. Chem. Soc.* **2003**, *125*, 10351−10361 and references therein. (b) Bryant, J. R.; Matsuo, T.; Mayer, J. M. *Inorg. Chem.* **2004**. *43*, 1587−1592.

(9) (a) Eberson, L.; Nilsson, M. *Acta Chem. Scand.* **1990**, *44*, 1062−1070. (b) Bockman, T. M.; Hubig, S. M.; Kochi, J. K. *J. Am. Chem. Soc.* **1998**, *120*, 2826−2830.

10.1021/ic048170q CCC: $30.25
Published on Web 03/08/2005

Chart 1

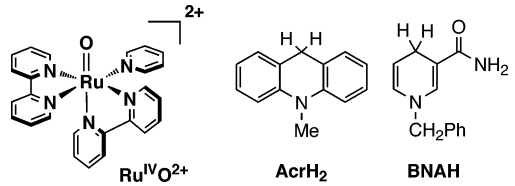

$Ru^{IV}O^{2+}$ $AcrH_2$ BNAH

Scheme 1. Possible Reaction Paths for Oxidation of NADH Analogs

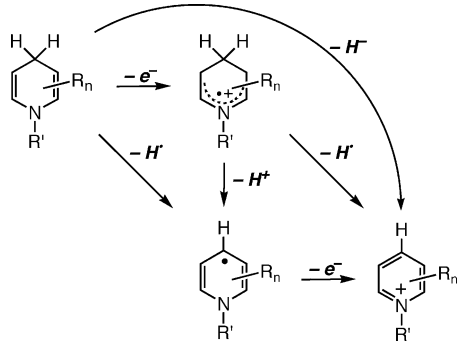

dihydroacridine ($AcrH_2$) and *N*-benzyl 1,4-dihydronicotinamide (BNAH; Chart 1).

Oxidation reactions of $\mathbf{Ru^{IV}O^{2+}}$ and other ruthenium(IV)−oxo complexes have been extensively studied both because of their wide range of substrates and because they utilize a variety of mechanisms. e^-, $H^\bullet$, and H^- transfer have each been implicated in various reactions of $\mathbf{Ru^{IV}O^{2+}}$.[6−10] Reduction of $\mathbf{Ru^{IV}O^{2+}}$ typically yields $[Ru^{III}(bpy)_2(py)(OH)]^{2+}$ ($\mathbf{Ru^{III}OH^{2+}}$) and $[Ru^{II}(bpy)_2(py)(H_2O)]^{2+}$ [$\mathbf{Ru^{II}(H_2O)^{2+}}$].[6] The properties of these materials including their redox potentials and acidities have been reported,[10] allowing detailed analysis of the reactions. Similarly, $AcrH_2$ and BNAH have been studied in detail as convenient analogues of NADH, 1,4-dihydronicotinamide adenine dinucleotide, and its phosphate form.[11] These are ubiquitous cofactors and the most common net hydride donors in biological systems.[12] NADH is usually converted to the corresponding cationic form, NAD^+, suggesting a preference for the two-electron mechanism of hydride transfer. However, previous studies have shown that NADH and its analogues can be oxidized by various mechanisms, including one-step H^- transfer; $H^\bullet$ followed by e^- transfer; and stepwise e^-, H^+, e^- transfers (Scheme 1).[12−14]

The abilities of $AcrH_2$ and BNAH to donate e^-, $H^\bullet$, and H^-—the redox potentials and homolytic and heterolytic C−H bond strengths—have been reported.[15−17] The affinity of $\mathbf{Ru^{IV}O^{2+}}$ to accept a hydrogen atom or a hydride ion can be evaluated using established thermochemical cycles[18] (see Table 1 below). Therefore, the oxidations of these NADH analogues by $\mathbf{Ru^{IV}O^{2+}}$ provide a rare opportunity to examine kinetic and mechanistic results in light of the thermochemistry of the possible pathways. We conclude that the reactions occur by hydrogen-atom transfer even though hydride transfer is roughly as favorable. This suggests that hydrogen-atom transfer is intrinsically as easy as or easier than hydride transfer.

Experimental Section

Materials. Acetonitrile (low-water, O_2-free, Burdick and Jackson) was dispensed from a steel keg plumbed directly into the drybox. CD_3CN was dried over CaH_2 for 2 days, vacuum transferred to P_2O_5, and stirred for 6 h. It was then transferred back to CaH_2, stirred for 30 min, and transferred to a sealable flask prior to use. 1,8-Diazabicylco[5.4.0]-indec-7-ene (DBU) was dried over KOH for 2 days under N_2, and distilled under reduced pressure. Other chemicals were obtained from commercial sources and used as received unless otherwise noted.

Ruthenium complexes except $\mathbf{Ru^{II}OH^+}$ were synthesized and assigned according to the previous reports.[6,10] $\mathbf{Ru^{II}OH^+}$ was obtained as a 1:1 mixture with $DBUH^+PF_6^-$ as follows: Under a N_2 atmosphere, $\mathbf{Ru^{II}(H_2O)^{2+}}$ was dissolved in MeCN containing 5 equiv of DBU. Et_2O was slowly added, and after 2 h, the brown precipitate was collected by filtration, rinsed with Et_2O to remove excess DBU, and dried in vacuo. UV/vis (MeCN): $\lambda_{max} = 503$ nm, $\epsilon = 5700\ M^{-1}\ cm^{-1}$. [The preparation of $\mathbf{Ru^{II}OH^+}$ in 100 mM sodium phosphate buffer (pH = 12) was unsuccessful because of the formation of some unidentifiable products, probably the result of OH^- addition to a pyridine ligand.]

10-Methyl-9,10-dihydroacridine ($AcrH_2$), 10-methylacridinium iodide ($AcrH^+I^-$),[13a] *N*-benzyl-1,4-dihydronicotinamide (BNAH), and *N*-benzylnicotinamidinium chloride (BNA^+Cl^-)[13,19] were synthesized following literature procedures. 10-Methylacridinium hexafluorophosphate ($AcrH^+PF_6^-$) was prepared by adding saturated aqueous KPF_6 to an aqueous solution of $AcrH^+I^-$. The corresponding isotopically labeled compounds ($AcrD_2$, $AcrD^+I^-$, and $AcrD^+PF_6^-$) were synthesized by the reduction of 10-methylacridone (AcrO) with $LiAlD_4$.[20] The D enrichments were found to be >98% for each material by the absence of the relevant peak in the ^1H NMR spectrum. All synthesized materials were characterized by ^1H NMR and UV−vis spectrometries.

(10) (a) Moyer, B. A.; Meyer, T. J. *Inorg. Chem*, **1981**, *20*, 436−444. (b) Dobson, J. C.; Helms, J. H.; Doppelt, P.; Sullivan B. P.; Hatfield, W. E.; Meyer, T. J. *Inorg. Chem*. **1989**, *28*, 2200−2204.

(11) The phosphate form is usually abbreviated as NADPH, but the term NADH is used for both species in this paper.

(12) (a) Mauzerall, D.; Westheimer, F. H. *J. Am. Chem. Soc*. **1955**, *77*, 2261−2264. (b) Stryer, L. *Biochemistry*, 3rd ed.; Freeman: New York, 1988; Chapter 17.

(13) (a) Roberts, R. M. G.; Ostovic, D.; Kreevoy, M. M. *Faraday Discuss. Chem. Soc*. **1982**, *74*, 257−265. (b) Yasui, S.; Ohno, A. *Bioorg. Chem*. **1986**, *14*, 70−78. (c) Fukuzumi, S. *Advances in Electron-Transfer Chemistry*; Mariano, P. S., Ed.; JAI Press: Greenwich, CT, 1992. (d) Chan, P. C.; Bielski, B. H. J. *J. Biol. Chem*. **1975**, *250*, 7266−7271.

(14) (a) Fukuzumi, S.; Tokuda, Y.; Kitano, T.; Okamoto, T.; Otera, J. *J. Am. Chem. Soc*. **1993**, *115*, 8960−8968. (b) Fukuzumi, S.; Okubo, K.; Tokuda, Y.; Suenobu, T. *J. Am. Chem. Soc*. **2000**, *122*, 4286−4294. (c) Fukuzumi, S.; Koumitsu, S.; Hironaka, K.; Tanaka, T. *J. Am. Chem. Soc*. **1987**, *109*, 305−316.

(15) (a) Zhu, X.-Q.; Li, H.-R.; Li, Q.; Ai, T.; Lu, J.-Y.; Yang, Y.; Cheng, J.-P. *Chem. Eur. J*. **2003**, *9*, 871−880. (b) Chen, J.-P.; Lu, Y.; Zhu, X.-Q.; Mu, L. *J. Org. Chem*. **1998**, *63*, 6108−6114.

(16) Handoo, K. L.; Cheng, J.-P.; Parker, V. D. *J. Am. Chem. Soc*. **1993**, *115*, 5067−5072.

(17) Ellis, W. W.; Raebiger, J. W.; Curtis, C. J.; Bruno, J. W.; DuBois, D. L. *J. Am. Chem. Soc*. **2004**, *126*, 2738−2743.

(18) For leading references to this kind of thermochemical analysis, see: (a) Bordwell, F. G.; Cheng, J.-P.; Ji, G.-Z.; Satish, A. V.; Zhang, X. *J. Am. Chem. Soc*. **1991**, *113*, 9790−9795. (b) Bordwell, F. G.; Cheng, J.-P.; Harrelson, J. A., Jr. *J. Am. Chem. Soc*. **1988**, *110*, 1229−1231. (c) Parker, V. D. *J. Am. Chem. Soc*. **1992**, *114*, 7458−7462; *J. Am. Chem. Soc*. **1993**, *115*, 1201 (correction). (d) Parker, V. D.; Handoo, K. L.; Roness, F.; Tilset, M. *J. Am. Chem. Soc*. **1991**, *113*, 7493−7498. (e) Mayer, J. M. In ref 1e; pp 1−43. (f) References 15−17.

(19) Anderson, A. G., Jr.; Berkelhammer, G. *J. Am. Chem. Soc*. **1958**, *80*, 992−999.

(20) Karrer, P.; Szabo, L.; Krishna, H. J. V.; Schwyzer, R. *Helv. Chim. Acta* **1950**, *33*, 294−300.

Instruments. ^{1}H NMR spectra were recorded on a Bruker AV-300 spectrometer at room temperature, and chemical shifts are reported as referenced to the peak from residual protio solvent. UV−vis spectra were recorded on a Hewlett-Packard 8453 diode-array spectrophotometer. Kinetic measurements were carried out with an OLIS RSM-1000 stopped-flow spectrophotometer. ESI-MS spectra were measured on a Bruker Esquire ion-trap mass spectrometer with an electrospray ionization source.

Typical Procedure for Oxidations. In a drybox, an organic substrate (1.5 mM) in CD_3CN (0.4 mL) and $\mathbf{Ru^{IV}O^{2+}}$ (1.5 mM) were quickly mixed in CD_3CN (0.4 mL), and the solution was monitored by ^{1}H NMR spectroscopy. To detect the products from the reaction of $AcrH_2$ with $\mathbf{Ru^{IV}O^{2+}}$, ESI-MS and UV−vis measurements were also employed. To determine the stoichiometry of $AcrH_2$ oxidation, yields were calculated on the basis of the intensities of the *N*-methyl groups in the ^{1}H NMR spectra. The concentration of $\mathbf{Ru^{IV}O^{2+}}$ was determined by rapid mixing with excess hydroquinone and measurement of the absorbance at 469 nm due to the formed $\mathbf{Ru^{II}(H_2O)^{2+}}$.[10]

Reaction of $AcrH^+$ with $Ru^{II}OH^+$. In a drybox, $AcrH^+PF_6^-$ (1.5 μmol) and $\mathbf{Ru^{II}OH^+}$ (0.75 μmol) were dissolved in CD_3CN (0.5 mL). A ^{1}H NMR spectrum was obtained after 1 h to identify the products. As a control experiment, it was shown independently with a similar procedure that $AcrH^+PF_6^-$ does not react with the $DBUH^+PF_6^-$ present in the isolated samples of $\mathbf{Ru^{II}OH^+}$.

Kinetic Measurements. Kinetic measurements were carried out under pseudo-first-order conditions ($[\mathbf{Ru^{IV}O^{2+}}]_0 \ll [AcrH_2]_0$, $[AcrD_2]_0$ or $[BNAH]_0$). Most measurements were done under anaerobic conditions: sample solutions were made up in a drybox and loaded in the stopped-flow apparatus minimizing contact with air. For measurements under aerobic conditions, sample solutions were made up in a drybox, put into an O_2-saturated flask equipped with an O_2 balloon, and gently stirred for 1 h prior to attachment to the stopped-flow apparatus. The spectral changes were analyzed using the global analysis software package SPECFIT (Spectrum Software Associates, Marlborough, MA), using an "A → B → C" model. The rate constants for the "A → B" phase were found to linearly depend on the initial concentration of $AcrH_2$ ($[AcrH_2]_0$), and these values are what are reported below. k_{obs} for the "B → C" phase did not show any simple dependence on the initial concentration of $AcrH_2$. $AcrH_2$ does not have any absorbance in the spectral region shown. The spectrum calculated for B is a composite of the individual spectra of all of the species that grow in during the first kinetic phase.

Results

Products of $AcrH_2$ Oxidation. Mixing acetonitrile solutions of 10-methyl-9,10-dihydroacridine ($AcrH_2$) and $\mathbf{Ru^{IV}O^{2+}}$ under anaerobic conditions causes a rapid color change from pale green to deep red, indicating the reduction of Ru^{IV} to Ru^{II}. ^{1}H NMR spectra of reactions in CD_3CN showed the dominant organic product to be 10-methylacridone (AcrO), whose identity was confirmed by ESI-MS ($M + H^+$, 210). Acridinium ($AcrH^+$) is observed as a minor product (<3% of AcrO); other organic products such as diacridinyl were not detected. These findings were surprising because the corresponding cationic species such as $AcrH^+$ are normally the products of oxidations of NADH analogues.[13,14] The ruthenium product was assigned as

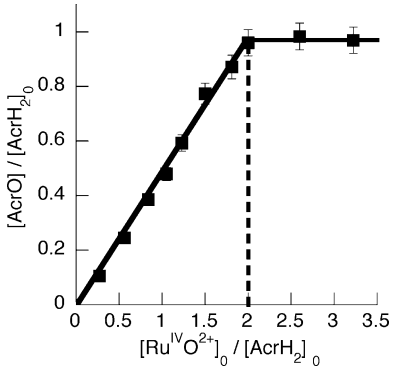

Figure 1. Plot of the yield of AcrO vs the ratio of initial concentrations of the reactants; $[AcrH_2]_0 = 2$ mM, $[\mathbf{Ru^{IV}O^{2+}}]_0 = 0.5-6$ mM. The amounts of AcrO and unreacted $AcrH_2$ were determined by ^{1}H NMR integration vs the $\mathbf{Ru^{II}(MeCN)^{2+}} + \mathbf{Ru^{IV}O^{2+}}$ present at the end of the reaction.

$\mathbf{Ru^{II}(MeCN)^{2+}}$ on the basis of its optical and ^{1}H NMR spectra, in particular the diagnostic resonance at $\delta = 9.4$ ppm due to the 6′-bipyridyl proton nearest to the pyridine ligand.[10b] $\mathbf{Ru^{II}(MeCN)^{2+}}$ is the typical product of solvolysis of $\mathbf{Ru^{II}(H_2O)^{2+}}$ or $\mathbf{Ru^{II}(ROH)^{2+}}$ in MeCN. The stoichiometry of this reaction was determined to be $[\mathbf{Ru^{IV}O^{2+}}]/[AcrH_2] = 2/1$ from the ^{1}H NMR titration as shown in Figure 1. The reaction is thus well described by the balanced equation

$$2\mathbf{Ru^{IV}O^{2+}} + AcrH_2 + 2MeCN \rightarrow 2\mathbf{Ru^{II}(MeCN)^{2+}} + AcrO + H_2O \quad (1)$$

In contrast, monitoring the reaction by UV−vis spectrophotometry with a stopped-flow instrument (under conditions where $[AcrH_2]_0 \approx 2[\mathbf{Ru^{IV}O^{2+}}]_0$) shows rapid formation of a substantial amount of $AcrH^+$ during the initial stage of the reaction ($\lambda_{max} = 358$, 420, and 444 nm; Figure 2a). The spectra also show growth of a peak at 474 nm, in the region of MLCT bands of Ru^{II} species. Spectra of the individual species are shown in Figure 2c. $\mathbf{Ru^{II}(H_2O)^{2+}}$ in MeCN has $\lambda_{max} = 469$ nm, and $\mathbf{Ru^{II}OH^+}$ has its MLCT band at 503 nm. Therefore, the 474-nm band suggests that $\mathbf{Ru^{IV}O^{2+}}$ has been converted into several Ru^{II} species in this stage. One of the species is likely to be $\mathbf{Ru^{II}OH^+}$, as this should be formed stoichiometrically with $AcrH^+$ upon a net hydride transfer from $AcrH_2$ to $\mathbf{Ru^{IV}O^{2+}}$.

The initial rapid reaction of $\mathbf{Ru^{IV}O^{2+}}$ and $AcrH_2$ is complete within a few seconds ($[AcrH_2]_0 = 1.3 \times 10^{-4}$ M, $[\mathbf{Ru^{IV}O^{2+}}]_0 = 6.3 \times 10^{-5}$ M, 25 °C). Over the following 10 min, the second kinetic phase is marked by a decrease in the absorbance at 358 nm due to $AcrH^+$ (Figure 2b). In addition, new bands at 400 and 440 nm appear, due to the formation of AcrO and $\mathbf{Ru^{II}(MeCN)^{2+}}$. This agrees with the products observed by ^{1}H NMR spectroscopy after ≥10 min (and higher reagent concentrations were used in the ^{1}H NMR experiments).

Reaction Path from $AcrH^+$ to AcrO. The observed conversion of $AcrH^+$ to AcrO was initially puzzling, because $AcrH^+$ does not react on this time scale with either the ruthenium starting material $\mathbf{Ru^{IV}O^{2+}}$ or the product $\mathbf{Ru^{II}(H_2O)^{2+}}$. This and the spectral changes suggested that $AcrH^+$ might react with transiently formed $\mathbf{Ru^{II}OH^+}$ to give

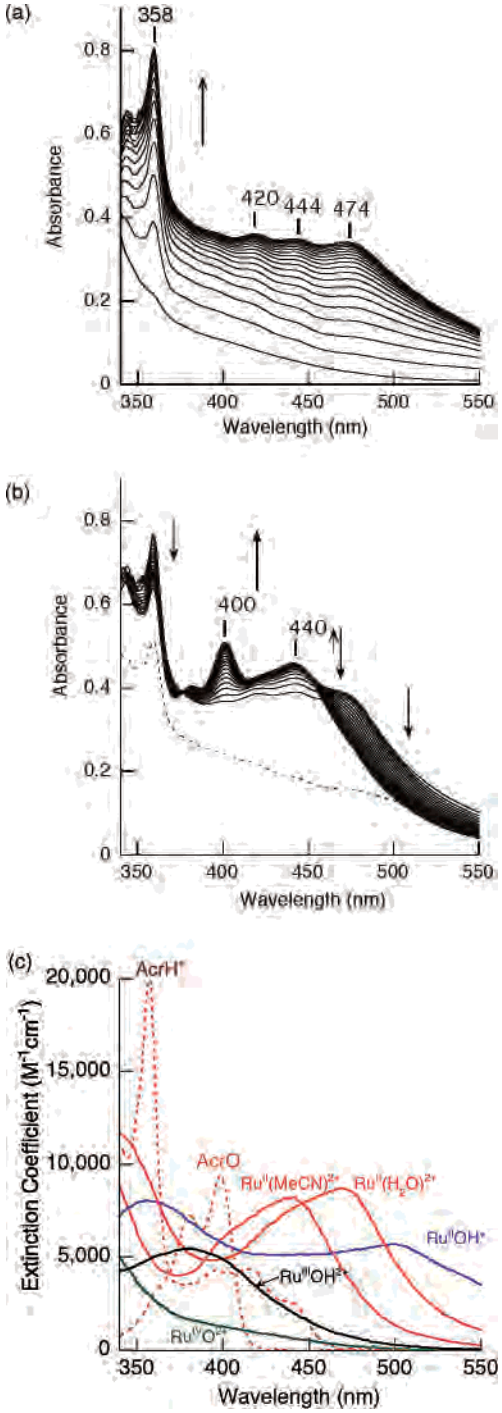

Figure 2. UV−vis spectra for the reaction of $AcrH_2$ (1.3×10^{-4} M) with $\mathbf{Ru^{IV}O^{2+}}$ (6.3×10^{-5} M) under anaerobic conditions in MeCN at 25 °C. (a) Initial stage, every 0.1 s over 2 s (taken at 1000 scan/s); (b) later stage, every 30 s over 570 s (taken at 1 scan/s). The spectrum indicted with a (b) dotted line was obtained after 1 s. (c) UV−vis spectra of isolated ruthenium complexes (solid lines) and acridine derivatives (dotted lines). $AcrH_2$ does not have any absorbance in this region.

AcrO and $\mathbf{Ru^{II}(MeCN)^{2+}}$. Thus, the reaction of $AcrH^+$ with $\mathbf{Ru^{II}OH^+}$ was attempted. $\mathbf{Ru^{II}OH^+}$ was generated by deprotonating $\mathbf{Ru^{II}(H_2O)^{2+}}$ with DBU in MeCN. Its optical spectrum has λ_{max} at 503 (MLCT), close to the value reported for this species in water (505 nm).[10a]

$AcrH^+PF_6^-$ reacts rapidly with $\mathbf{Ru^{II}OH^+}$ at room temperature in CD_3CN to give AcrO and $AcrH_2$ in a 1:1 ratio,

Scheme 2. Suggested Mechanism of Acridone (AcrO) Formation from Acridinium, Illustrated for the Deuterated Material ($AcrD^+$): (a) Nucleophilic Attack of $Ru^{II}OH^+$ on $AcrD^+$ to Give Alcohol or Alkoxide and (b) Hydride Transfer from Alcohol or Alkoxide to $AcrD^+$

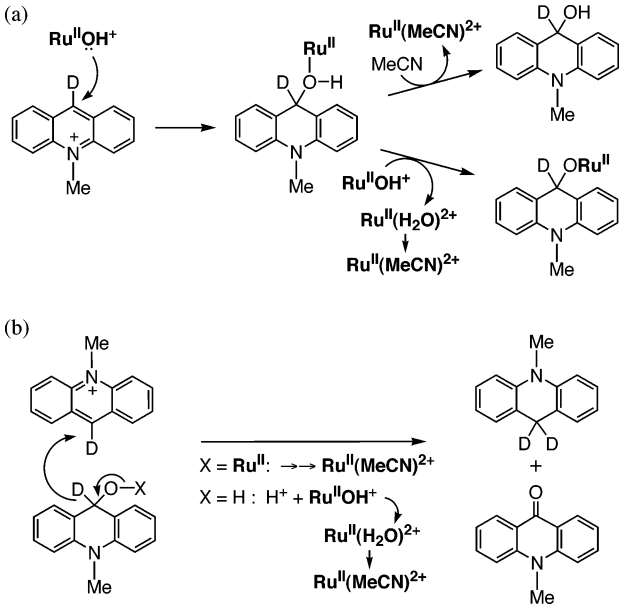

together with $\mathbf{Ru^{II}(MeCN)^{2+}}$ (by ^1H NMR spectroscopy) (eq 2).

$$2\mathbf{Ru^{II}OH^+} + 2AcrH^+ + 2MeCN \rightarrow 2\mathbf{Ru^{II}(MeCN)^{2+}} + AcrO + AcrH_2 + H_2O \quad (2)$$

This reaction is quite similar to the hydroxide-induced disproportionation of $AcrH^+$ to AcrO and $AcrH_2$ described in alkaline aqueous solutions.[21] Addition of OH^- to the electron-deficient C-9 position of $AcrH^+$ forms the alcohol intermediate AcrH(OH), which then undergoes net hydride transfer to another molecule of $AcrH^+$ to form AcrO and $AcrH_2$. Presumably, $\mathbf{Ru^{II}OH^+}$ can also serve as the nucleophile and base in a similar mechanism [the pK_a of $\mathbf{Ru^{II}(H_2O)^{2+}}$ in water is 10.8[10c]]. When the deuterated $AcrD^+$ was employed as a reactant, $AcrD_2$ was formed. These data implicate a mechanism of initial $\mathbf{Ru^{II}OH^+}$ addition to the C-9 position of $AcrH^+$ to give the alcohol AcrH(OH) (upon Ru dissociation) and/or the alkoxide $\mathbf{Ru^{II}(OAcrH)^+}$ (upon deprotonation). These transients are good hydride donors and reduce $AcrH^+$ to $AcrH_2$, forming AcrO (Scheme 2; illustrated for the deuterated material).

Initial Yield of $AcrH^+$. A key question is whether the acridinium transiently formed from $AcrH_2$ and $\mathbf{Ru^{IV}O^{2+}}$ is produced via direct hydride transfer or via a multistep mechanism. The yield of $AcrH^+$ at the end of the first kinetic phase can be estimated from the optical spectra in Figure 2a. The subsequent decay of $AcrH^+$ (Figure 2b) does not complicate this analysis because it occurs on a much slower time scale (2 vs 500 s). The spectrum at the end of the first kinetic phase was simulated by combining the spectra of

(21) (a) Clark, J.; Bakavoli, M. *J. Chem. Soc., Perkin Trans 1* **1977**, 1966−1968. (b) Shinkai, S.; Tsuno, T.; Manabe, O. *J. Chem. Soc., Perkin Trans. 2* **1984**, 661−665. (c) Bunting, J. W.; Kauffman, G. M. *Can. J. Chem.* **1984**, 62, 729−735.

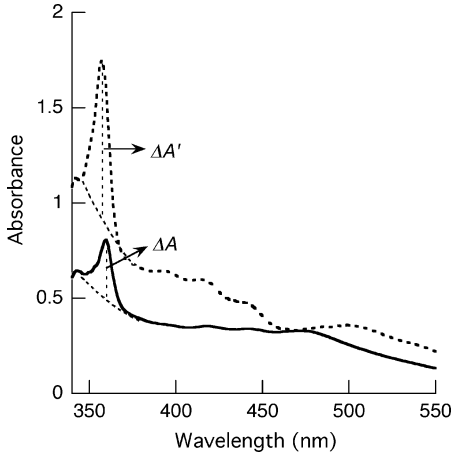

Figure 3. Comparison of observed and simulated spectra. The observed spectrum (solid line) was collected 1.6 s after mixing ($[AcrH_2]_0 = 1.3 \times 10^{-4}$ M, $[\mathbf{Ru^{IV}O^{2+}}]_0 = 6.3 \times 10^{-5}$ M) at 25 °C under a N_2 atmosphere. The simulated spectrum (dotted line) is the sum of the spectra of $AcrH^+$ and $\mathbf{Ru^{II}OH^+}$ (both 6.3×10^{-5} M), the products of one-step hydride transfer.

$AcrH^+$ and $\mathbf{Ru^{II}OH^+}$ at the appropriate concentrations, as shown in Figure 3. The observed spectrum has lower absorbance than the simulated one, as is particularly evident in the sharp band at 358 nm due to $AcrH^+$. According to the intensity ratio of this peak ($\Delta A/\Delta A'$), the yield of transiently formed $AcrH^+$ is 40−50%. Thus formation of $AcrH^+$ is not quantitative and must compete with other reaction paths. In other words, the reaction cannot proceed solely by initial one-step hydride transfer.

Kinetic Measurements for the Initial Phase. The kinetics of $\mathbf{Ru^{IV}O^{2+}}$ oxidation of $AcrH_2$ were monitored under anaerobic conditions with a stopped-flow apparatus. Pseudo-first-order conditions, $[AcrH_2]_0 \gg [\mathbf{Ru^{IV}O^{2+}}]_0$, were used for simple analysis. The spectral changes under the pseudo-first-order conditions were also similar to those observed for $[AcrH_2]_0 \approx [\mathbf{Ru^{IV}O^{2+}}]_0$ (shown in Figure 2a). Upon the mixing of the reactants, an increase in the absorbance at 358 nm, the indicator of $AcrH^+$ formation, was observed. The typical growth of the absorbance is shown in Figure 4a. This time course was a typical first-order process to give the apparent first-order rate constant k_{obs}. The rate constant depends linearly on the initial concentration of $AcrH_2$ (Figure 4b), indicating that the initial stage is a bimolecular reaction process between $AcrH_2$ and $\mathbf{Ru^{IV}O^{2+}}$. The slope of this plot gives the second-order rate constant $k = (5.7 \pm 0.3) \times 10^3$ M^{-1} s^{-1}. Oxidation of $AcrD_2$ (isotopic purity >98%) reveals a large kinetic isotope effect: $k_{AcrH_2}/k_{AcrD_2} = 12 \pm 1$ (Figure 4). An Eyring plot of second-order rate constants determined from 5 to 45 °C yields $\Delta H^{\ddagger} = 5.3 \pm 0.3$ kcal mol^{-1} and $\Delta S^{\ddagger} = -23 \pm 1$ cal mol^{-1} K^{-1}. The spectral changes after the initial phase are sufficiently complicated that a clear assignment of the process or the formed species has not been possible. Reactions occurring over this time period include the conversion of $AcrH^+$ to AcrO (see above) and the solvolysis of $\mathbf{Ru^{II}(H_2O)^{2+}}$ to $\mathbf{Ru^{II}(MeCN)^{2+}}$.

Kinetic measurements were also made with solutions saturated with O_2 (1 atm, $[O_2] = 8$ mM[22]). Both the rates

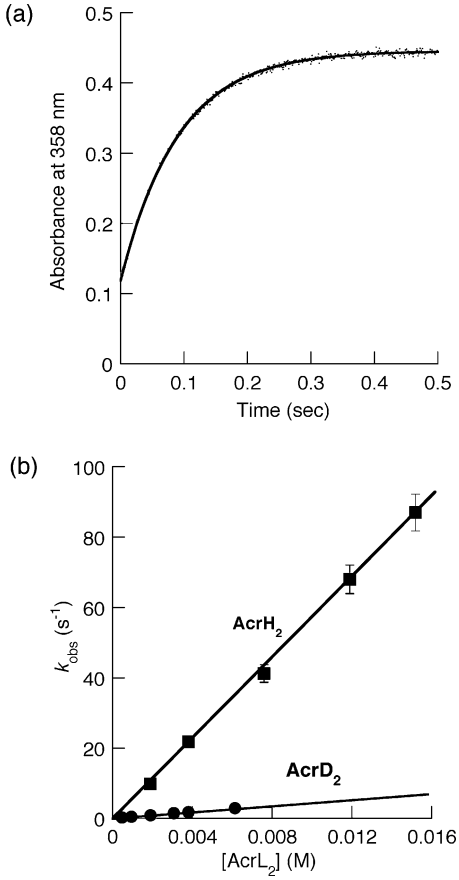

Figure 4. (a) Absorbance change at 358 nm in the initial phase of $AcrH_2$ oxidation by $\mathbf{Ru^{IV}O^{2+}}$ at 25 °C in MeCN under anaerobic conditions; $[AcrH_2]_0 = 2.0 \times 10^{-3}$ M, $[\mathbf{Ru^{IV}O^{2+}}] = 2.0 \times 10^{-5}$ M. The solid line is the fitting line of the first-order kinetics. (b) Pseudo-first-order plot for the kinetics of $AcrL_2$ (L = H, D) with $\mathbf{Ru^{IV}O^{2+}}$ at 25 °C in MeCN under anaerobic conditions.

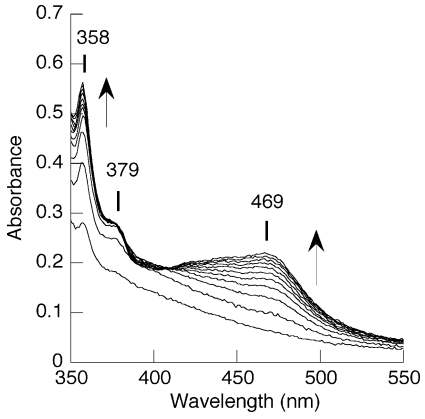

Figure 5. Transient UV−vis spectra (collected every 10 ms over 100 ms) for the reaction of $AcrH_2$ with $\mathbf{Ru^{IV}O^{2+}}$ under O_2-saturated conditions at 25 °C in MeCN. $[AcrH_2]_0 = 3.0 \times 10^{-3}$ M, $[\mathbf{Ru^{IV}O^{2+}}]_0 = 3.5 \times 10^{-5}$ M.

and the products are strongly affected by the presence of dioxygen. The transient spectra (Figure 5) reveal new absorbance features at 379 and 469 nm. Through a comparison with the spectra of authentic samples shown in Figure 2c, the 379-nm feature can be attributed to the accumulation of the ruthenium(III) hydroxide, $\mathbf{Ru^{III}OH^{2+}}$, and 469 nm is the λ_{max} for the MLCT band of $\mathbf{Ru^{II}(H_2O)^{2+}}$. The second-order rate constant for the first phase under O_2 was found to be $(2.7 \pm 0.2) \times 10^4$ M^{-1} s^{-1}. This value is 5 times larger

(22) Achord, J. M.; Hussey, C. L. *Anal. Chem.* **1980**, *52*, 601.

than that under anaerobic conditions. Such acceleration under aerobic conditions has also been observed in the oxidation of cumene by $\mathbf{Ru^{IV}O^{2+}}$.[8] The ruthenium complexes are all stable to O_2 on this time scale, so O_2 must be intercepting an organic intermediate, most likely the acridinyl radical AcrH$^\bullet$. The yield of AcrH$^+$ was also estimated to be ~30% in the manner described above. This suggests that O_2 inhibits the formation of AcrH$^+$ by trapping AcrH$^\bullet$ (see below).

Oxidation of BNAH by $\mathbf{Ru^{IV}O^{2+}}$. *N*-Benzyl-1,4-dihydronicotinamide (BNAH) is also rapidly oxidized by $\mathbf{Ru^{IV}O^{2+}}$ in CD_3CN under anaerobic conditions. UV−vis spectra obtained using a stopped-flow apparatus show growth of a composite MLCT band for Ru^{II} species at 476 nm. This is at slightly longer wavelength than observed in the $AcrH_2$ oxidation, suggesting a larger contribution from $\mathbf{Ru^{II}OH^+}$ ($\lambda_{max} = 503$ nm). ^{1}H NMR spectra of reaction mixtures show the formation of both $\mathbf{Ru^{II}(MeCN)^{2+}}$ and $\mathbf{Ru^{II}OH^+}$, confirming the optical assignment. The NMR spectra also show BNA$^+$ (60−75% yield) and several unidentified products probably derived from BNAH. A decrease in the concentration of BNA$^+$ occurs over 24 h, accompanied by the appearance of a considerable amount of insoluble materials. In water, nucleophilic addition of OH^- to the pyridinium ring of BNA$^+$ is reported to be slower than addition to AcrH$^+$.[23] This is consistent with the observation of both BNA$^+$ and $\mathbf{Ru^{II}OH^+}$ in reaction mixtures, unlike the $AcrH_2$ case.

Kinetic measurements under a N_2 atmosphere indicated a second-order rate constant $k = (7.0 \pm 0.4) \times 10^4$ M^{-1} s^{-1}. This is 1 order of magnitude larger than that for $AcrH_2$ oxidation. An Eyring plot of rate constants measured from 5 to 45 °C yields $\Delta H^\ddagger = 3.9 \pm 0.2$ kcal mol^{-1} and $\Delta S^\ddagger = -23 \pm 2$ cal mol^{-1} K^{-1}.

Discussion

Mechanism of $\mathbf{AcrH_2}$ and BNAH Oxidations by $\mathbf{Ru^{IV}O^{2+}}$. The first observed products of $AcrH_2$ and BNAH oxidations by $\mathbf{Ru^{IV}O^{2+}}$ are the corresponding cationic species, AcrH$^+$ and BNA$^+$. This represents net hydride transfer, which at first glance suggested a mechanism of one-step hydride transfer. Hydride transfer is a well-documented mechanism for oxidations of NADH and its analogues by various metal and organic oxidants.[12−14] $\mathbf{Ru^{IV}O^{2+}}$ has been shown in a few cases to abstract hydride from substrates (e.g., formate[24b]). However, the yields of AcrH$^+$ and BNA$^+$ are not quantitative, and both cations are stable on the time scale of the yield measurement, indicating that hydride transfer cannot be the sole pathway. The kinetics of $AcrH_2$ oxidation are significantly affected in the presence of O_2, suggesting the presence of a carbon radical intermediate, most likely AcrH$^\bullet$ formed by hydrogen-atom abstraction. In addition, as shown in Figure 6 below, the rate constants for $AcrH_2$ and BNAH oxidations correlate very well with other

Scheme 3. Proposed Mechanism of $AcrH_2$ Oxidation by $Ru^{IV}O^{2+}$ under Anaerobic Conditions

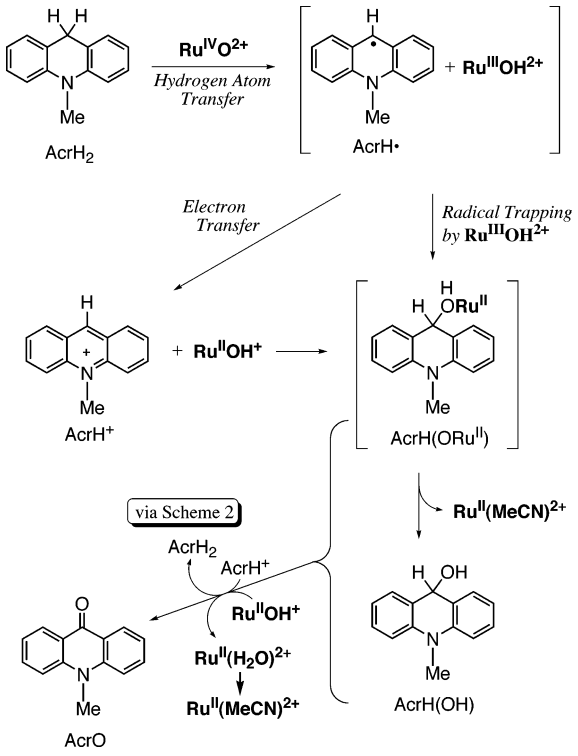

oxidations of C−H bonds by $\mathbf{Ru^{IV}O^{2+}}$ that have been shown to occur by hydrogen-atom transfer. These findings are most consistent with an oxidation mechanism involving the initial hydrogen-atom (H$^\bullet$) transfer from the substrates to $\mathbf{Ru^{IV}O^{2+}}$.

The proposed mechanism, shown in Scheme 3, starts with $\mathbf{Ru^{IV}O^{2+}}$ abstracting H$^\bullet$ from $AcrH_2$ to form $\mathbf{Ru^{III}(OH)^{2+}}$ and an acridinyl radical, AcrH$^\bullet$. AcrH$^\bullet$ is then rapidly oxidized by one of two paths. Electron transfer from AcrH$^\bullet$ to $\mathbf{Ru^{III}OH^{2+}}$ is quite downhill [$E°$(AcrH$^+$) = −0.19 V vs NHE in MeCN[25] and $E°(\mathbf{Ru^{III/II}OH^{2+/+}}) \approx +1$ V (see below)] and the reagents have small intrinsic barriers.[26] Therefore, electron transfer to give AcrH$^+$ and $\mathbf{Ru^{III}OH^{2+}}$ should be very fast.[27] BNA$^\bullet$ is even easier to oxidize [$E°$(BNA$^+$) = −0.89 V vs NHE in MeCN[25]], and it appears that a larger fraction of BNA$^\bullet$ radicals are oxidized by electron transfer to BNA$^+$. Alternatively, AcrH$^\bullet$ can be trapped by C−O bond formation with $\mathbf{Ru^{III}OH^{2+}}$ [or potentially $\mathbf{Ru^{IV}O^{2+}}$ (not shown in the scheme)].[8] C−O bond formation was found to be a particularly facile process in oxidations of alkylaromatic and allylic hydrocarbons by $\mathbf{Ru^{IV}O^{2+}}$, in some cases occurring efficiently within the solvent cage.[8,28] Electron-transfer and C−O bond-formation paths are apparently close in rate given that the observed initial yield of AcrH$^+$ is 40−50%. C−O bond formation

(23) Bunting, J. W. *Bioorg. Chem.* **1991**, *19*, 456−491.
(24) (a) Thompson, M. S.; Meyer, T. J. *J. Am. Chem. Soc.* **1982**, *104*, 4106−4115. (b) Roecker, L.; Meyer, T. J.; *J. Am. Chem. Soc.* **1986**, *108*, 4066−4073. (c) Roecker, L.; Meyer, T. J.; *J. Am. Chem. Soc.* **1987**, *109*, 746−754.
(25) Converted to vs NHE based on the reported value[14c] vs SCE.
(26) Eberson L. *Electron Transfer in Organic Chemistry*; Springer-Verlag: New York, 1987. $\lambda \approx 5-12$ kcal mol^{-1} for X/X$^+$ couples involving organic molecules of this size in MeCN and $\lambda \approx 10-50$ kcal mol^{-1} for Ru^{II}/ Ru^{III} couples (pp 51−53).
(27) With $E = 1.2$ V and $\lambda \approx 10-30$ kcal mol^{-1} (0.4−1.3 eV)[26] for AcrH$^\bullet$ + $\mathbf{Ru^{III}OH^{2+}}$, the adiabatic Marcus equation indicates that electron transfer should occur at close to the diffusion limit.
(28) Stultz, L. K.; Huynh, M. H. V.; Binstead, R. A.; Curry, M.; Meyer, T. J. *J. Am. Chem. Soc.* **2000**, *122*, 5984−5996.

yields the alcohol AcrH(OH), in either its free or ruthenium-complexed form. This is then oxidized to the observed ketone AcrO by $AcrH^+$, as described in Scheme 2.

Under aerobic conditions, free $AcrH^•$ is trapped by O_2 ($[O_2] = 8$ mM; $k = 4.3 \times 10^9$ M^{-1} s^{-1} at 25 °C)[29] as well as by electron transfer and C−O bond formation. Thus less of the reaction proceeds by electron transfer, so that less $AcrH^+$ is formed (its yield is reduced from 40−50% to ∼30%) and more $\mathbf{Ru^{III}OH^{2+}}$ accumulates (as observed in the optical spectra as a shoulder at 379 nm). $\mathbf{Ru^{III}OH^{2+}}$ can also be formed by comproportionation of $\mathbf{Ru^{II}(H_2O)^{2+}}$ and $\mathbf{Ru^{IV}O^{2+}}$.[30] Under dioxygen, the mechanism is substantially more complicated because AcrH(OO•), $\mathbf{Ru^{IV}O^{2+}}$, and $\mathbf{Ru^{III}OH^{2+}}$ can all abstract H• from $AcrH_2$ and be involved in autoxidation radical chains.

It is possible that a portion of the $AcrH_2$ oxidation, ≤30%, could occur by hydride transfer competitive with H• transfer. There would need to be two pathways to $AcrH^+$ to explain the change in yield with added O_2, and the rate constant for H^- transfer would have to be coincidentally close to that for H• transfer. Although the data do not exclude this possibility, there is also no reason to invoke such a second pathway. The entropies of activation for $AcrH_2$ and BNAH oxidations, both −23 cal mol^{-1} K^{-1}, also seem most consistent with a hydrogen-atom transfer mechanism. Oxidations of xanthene and cyclohexene by $\mathbf{Ru^{IV}O^{2+}}$, which occur by H-atom transfer, have $\Delta S^‡ = -30 \pm 5$ and -34 ± 3.4 cal mol^{-1} K^{-1},[8a] respectively, whereas 2-propanol oxidation by hydride transfer has a more negative $\Delta S^‡$ of -42 ± 5 cal mol^{-1} K^{-1}.[24a] Presumably H^- transfer involves more charge transfer and therefore a more ordered transition state.

An alternative mechanism of initial rate-limiting electron transfer from $AcrH_2$ to $\mathbf{Ru^{IV}O^{2+}}$ is ruled out by the large kinetic isotope effect (KIE) for oxidation of $AcrD_2$: $k_{AcrH_2}/k_{AcrD_2} = 12 \pm 1$.[31] C−H bond cleavage in $AcrH_2$ must be involved in the rate-limiting step. The isotope effect could be consistent with rate-limiting proton transfer after preequilibrium electron transfer,[9] but $\mathbf{Ru^{IV}O^{2+}}$ is in general a poor outersphere electron-transfer oxidant.[32] The observed KIE is larger than that observed previously in NADH analogue oxidations[33] but not unusual for reactions of $\mathbf{Ru^{IV}O^{2+}}$.[6,8,24,28,30] Hydride transfers to $\mathbf{Ru^{IV}O^{2+}}$ from alcohols or formate exhibit k_H/k_D values from 9 to 50;[24] KIEs for hydrogen-atom transfers to $\mathbf{Ru^{IV}O^{2+}}$ are large (dihydroanthracene, ≥ 35; cyclohexene, 21) but smaller for H-atom transfers to $\mathbf{Ru^{III}OH^{2+}}$.[8,28] In our view, the magnitude of k_H/k_D cannot in any simple way be used to distinguish among proton, hydrogen atom, and hydride transfer mechanisms.

Thermochemical Hydrogen-Atom and Hydride Affinities. Previous work has provided the thermodynamics for removal of H• or H^- from $AcrH_2$, BNAH, and the ruthenium complexes (Table 1). These values are derived primarily from electrochemical and acidity measurements and converted to bond dissociation enthalpies (BDEs) and hydride affinities $\Delta G°(H^-)$ using thermochemical cycles.[18] For the NADH analogues, the BDEs come from a recent study by Zhu et al.[15] Table 1 gives the free energies of hydride transfer from Parker and co-workers,[16] as well as a more recent significantly lower value of $\Delta G°(H^-)$ for BNAH from Curtis et al.[17]

Table 1. Homolytic and Heterolytic X−H Bond Dissociation Energies (kcal mol^{-1})

hydrogen-atom transfer	BDE	ref
$\mathbf{Ru^{III}OH^{2+}} \rightarrow \mathbf{Ru^{IV}O^{2+}} + H^•$	84 ± 2	8
$\mathbf{Ru^{II}(H_2O)^{2+}} \rightarrow \mathbf{Ru^{III}OH^{2+}} + H^•$	82 ± 2	8
$AcrH_2 \rightarrow AcrH^• + H^•$	73.7 ± 1.0	15a
$BNAH \rightarrow BNA^• + H^•$	67.9 ± 1.0	15a
hydride transfer	**$\Delta G°(H^-)$**	**ref**
$\mathbf{Ru^{II}OH^+} \rightarrow \mathbf{Ru^{IV}O^{2+}} + H^-$	89 ± 5	*a*
$AcrH_2 \rightarrow AcrH^+ + H^-$	83 ± 1[b]	16
$BNAH \rightarrow BNA^+ + H^-$	72 ± 1[b]	16
	59 ± 2	17

[a] See text. [b] $\Delta H°(H^-)$ values of 81.1 ($AcrH_2$) and 64.2 kcal mol^{-1} (BNAH) have been reported by Zhu et al.[15a]

Scheme 4. Hydride Affinity of $Ru^{IV}O^{2+}$ in MeCN[a]

$$\mathbf{Ru^{IV}O^{2+}} + H^• \rightarrow \mathbf{Ru^{III}OH^{2+}} \qquad \Delta G° = -79.4$$

$$\mathbf{Ru^{III}OH^{2+}} + e^- \rightarrow \mathbf{Ru^{II}OH^{2+}} \qquad E° \cong +1.0\ V$$

$$H^- \rightarrow H^• + e^- \qquad E° \cong -0.6\ V\ [16]$$

$$\mathbf{Ru^{IV}O^{2+}} + H^- \rightarrow \mathbf{Ru^{II}OH^+} \qquad \Delta G°(H^-) = -89 \pm 5$$

[a] Free energies in kcal mol^{-1}; potentials in MeCN vs NHE. $\Delta G°$ (kcal mol^{-1}) = 23.06ΔE (V).

For the ruthenium complexes, we have previously derived the bond dissociation enthalpies (BDEs)[8] from published aqueous electrochemical data.[10] It is assumed, as is common, that BDEs are, to a good approximation, independent of solvent.[34] The free energy for hydrogen-atom loss is taken as the BDE plus $T\Delta S°(H^•)$ (≈ −4.6 kcal mol^{-1}).[18d,35] Following the approach of Parker,[16] the hydride affinity is this $\Delta G°(H^•)$ plus a redox potential ($H^- \equiv H^• + e^-$), as shown in Scheme 4. The redox potential of $\mathbf{Ru^{III}OH^{2+}}$ in MeCN has not been previously reported. In our hands, cyclic voltammograms of $\mathbf{Ru^{III}OH^{2+}}$ are not reversible; the potential in the scheme is estimated from $E_{p,a} = +1.12$ V.[36]

Correlation of Rate Constants and BDEs. We and others have shown that a number of metal oxidants can abstract a hydrogen atom from a C−H bond.[2,5,8a] Over a series of similar H-atom transfer reactions, there is typically a good correlation of rate constants with C−H BDEs.[2] This is typical of organic radical chemistry as well.[2] Recently, we reported

(29) Pestovsky, O.; Bakac, A.; Espenson, J. H. *J. Am. Chem. Soc.* **1998**, *120*, 13422−13428.
(30) Binstead, R. A.; Stultz, L. K.; Meyer, T. J. *Inorg. Chem.* **1995**, *34*, 546−551.
(31) In the oxidation of $AcrH_2$, the visible band due to $AcrH_2^{•+}$ (λ_{max} = 650 nm)[14a] is not observed.
(32) Lebeau, E. L.; Binstead, R. A.; Meyer, T. J. *J. Am. Chem. Soc.* **2001**, *123*, 10535−10544.
(33) Ostovic, D.; Roberts, R. M. G.; Kreevoy, M. M. *J. Am. Chem. Soc.* **1983**, *105*, 7629−7631.
(34) Compare: (a) Pratt, D. A.; Dilabio, G. A.; Mulder, P.; Ingold, K. U. *Acc. Chem. Res.* **2004,** *37*, 334−340. (b) See also ref 18.
(35) This calculation assumes that $S°(\mathbf{Ru^{IV}O^{2+}}) \approx S°(\mathbf{Ru^{III}OH^{2+}})$.
(36) $E°\{cis\text{-}[Ru(bpy)_2(py)Cl]^{2+/+}\}$ is ca. +0.98 V vs NHE as estimated from a figure in: Ellis, C. D.; Murphy, W. R., Jr.; Meyer, T. J. *J. Am. Chem. Soc.* **1981**, *103*, 7480−7483.

such a correlation for the oxidations of a series of alkyl aromatic and allylic C−H bonds by $\mathbf{Ru^{IV}O^{2+}}$.[8a] Using the BDEs in Table 1, $AcrH_2$ and BNAH can be added to this correlation as shown in Figure 6.[37] The rate constants for $AcrH_2$ and BNAH oxidations fit the correlation quite well. This is strong evidence that all of these compounds, including the NADH analogues, react by a common hydrogen-atom transfer mechanism.

Relative Intrinsic Barriers for Hydrogen-Atom and Hydride Transfer. The free energy changes for hydrogen-atom and hydride transfer from $AcrH_2$ to $\mathbf{Ru^{IV}O^{2+}}$, eqs 3 and 4, are readily derived from the data in Table 1. (It is assumed, as is common, that $\Delta G° \approx \Delta H°$ for hydrogen-atom transfer reactions.[38])

Hydrogen-atom transfer

$$\mathbf{Ru^{IV}O}^{+} + AcrH_2 \rightarrow \mathbf{Ru^{III}OH^{2+}} + AcrH^{\bullet} \qquad (3)$$

$\Delta G° =$

-10 ± 2 kcal mol^{-1} (-16 ± 3 kcal mol^{-1} for BNAH)

Hydride transfer

$$\mathbf{Ru^{IV}O^{2+}} + AcrH_2 \rightarrow \mathbf{Ru^{II}OH}^{+} + AcrH^{+} \qquad (4)$$

$\Delta G° =$

-6 ± 5 kcal mol^{-1} (-17 or -30 kcal mol^{-1} for BNAH)

In the case of $AcrH_2$ oxidation, hydrogen-atom transfer to $\mathbf{Ru^{IV}O^{2+}}$ ($\Delta G° = -10 \pm 2$ kcal mol^{-1}) might be slightly more exoergic than the alternative hydride transfer mechanism (-6 ± 5 kcal mol^{-1}), although the uncertainties are significant. Given the common assumption that NADH analogues are good hydride donors, it is surprising that, for $AcrH_2$, H$^{\bullet}$ transfer is comparable to or perhaps more favorable than H$^-$ transfer. For the oxidation of BNAH, there might be a substantial thermodynamic preference for hydride transfer.

The mechanistic studies implicate a pathway of initial hydrogen-atom transfer, not hydride transfer from $AcrH_2$. This could be due in part to a small thermochemical preference for H$^{\bullet}$ over H$^-$ transfer, $\Delta\Delta G° = -4 \pm 6$ kcal mol^{-1}. The analysis also suggests that hydrogen-atom transfer cannot be intrinsically a much more difficult reaction than hydride transfer, or else that preference would overcome the small thermochemical bias. In the context of a Marcus-theory analysis, hydrogen-atom transfer appears to have a comparable or smaller *intrinsic barrier*. (For applications of Marcus theory to H$^{\bullet}$ and H$^-$ transfer reactions, see refs 5c and 39). We have previously suggested that hydride transfer is intrinsically much less facile than electron transfer, based on a study of alkylaromatic oxidations by $[Mn_2(\mu\text{-}O)_2(phen)_4]^{4+}$.[5c] The manganese complex oxidizes *para*-methoxytoluene by electron transfer even though hydride transfer is 24 kcal mol^{-1} more favorable. H$^{\bullet}$ transfer could be easier than H$^-$ transfer because of the smaller solvent (outer-sphere) reorganization upon transfer of a neutral atom. Hammes-Schiffer et al. have calculated a lower solvent reorganization for transfer of H$^{\bullet}$ vs e$^-$ transfer in an iron system.[40] More studies are required to test the generality of these conclusions, but they suggest a rationale for why there has at times been controversy about one-step hydride transfer mechanism.[12−14,23,41] When a system has a choice of pathways that are thermodynamically reasonable, e$^-$ or H$^{\bullet}$ transfer will likely occur in preference. Only when there is a large thermochemical preference for hydride transfer should this pathway be favored. One example is the oxidation of formate by $\mathbf{Ru^{IV}O^{2+}}$ by hydride transfer, for which Meyer et al. have shown there to be a large thermochemical preference for H$^-$ over H$^{\bullet}$ transfer ($\Delta\Delta G° = -27.9$ kcal mol^{-1}).[24b]

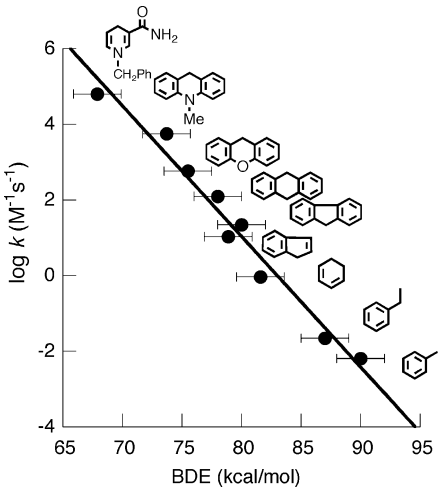

Figure 6. Plot of rate constants for oxidations by $\mathbf{Ru^{IV}O^{2+}}$ vs C−H bond energies (BDEs).

Conclusions

The NADH analogues 10-methyl-9,10-dihydroacridine ($AcrH_2$) and *N*-benzyl 1,4-dihydronicotinamide (BNAH) are rapidly oxidized by *cis*-$[Ru^{IV}(bpy)_2(py)(O)]^{2+}$ ($\mathbf{Ru^{IV}O^{2+}}$). Thermochemical analysis indicates that the reactions could proceed through either initial hydrogen-atom transfer ($\Delta G° = -10 \pm 2$ kcal mol^{-1} for $AcrH_2$ oxidation) or initial hydride transfer ($\Delta G° = -6 \pm 5$ kcal mol^{-1} for $AcrH_2$ oxidation).

In the reaction of $AcrH_2$ with $\mathbf{Ru^{IV}O^{2+}}$, the first kinetic phase exhibits bimolecular kinetics and a large primary isotope effect ($k_{AcrH_2}/k_{AcrD_2} = 12 \pm 1$). $AcrH^+$ is formed in this step but in only 40−50% yield, indicating that one-step hydride transfer cannot be the sole mechanism. $AcrH^+$ is then more slowly converted into AcrO and $AcrH_2$ via nucleophilic attack of $\mathbf{Ru^{II}OH}^{+}$ on the electrophilic C-9 of

(37) The rate constants for $AcrH_2$ and BNAH in Figure 6 have not been corrected for the stoichiometry of the reactions (moles of $\mathbf{Ru^{IV}O^{2+}}$ consumed per H$^{\bullet}$ transfer) because of the complexity of the product mix of the reactions.

(38) (a) Blanksby, S. J.; Ellison, G. B. *Acc. Chem. Res.* **2003**, *36*, 255−263. For an exception, see: (b) Mader, E. A.; Larsen, A. S.; Mayer, J. M. *J. Am. Chem. Soc.* **2004**, *126*, 8066−8067.

(39) Schindele, C.; Houk, K. N.; Mayr, H. *J. Am. Chem. Soc.* **2002**, *124*, 11208−11214.

(40) Iordanova, N.; Decornez, H.; Hammes-Schiffer, S. *J. Am. Chem. Soc.* **2001**, *123*, 3723−3733.

(41) (a) Miller, L. L.; Valentine, J. R. *J. Am. Chem. Soc.* **1988**, *110*, 3982−3989 and references therein. (b) Coleman, C. A.; Rose, J. G.; Murray, C. J. *J. Am. Chem. Soc.* **1992**, *114*, 9755−9762. (c) Ohno, A. *Bull. Chem. Soc. Jpn.* **1998**, *71*, 2041−2050.

$AcrH^+$. The data are most consistent with a mechanism of initial hydrogen-atom transfer, as found for oxidations of alkylaromatic and allylic C−H bonds by $\mathbf{Ru^{IV}O^{2+}}$.[8] Rate constants for $AcrH_2$ and BNAH oxidation correlate well with the previously established relation of k with C−H bond strength (Figure 6). In addition, the oxidation of $AcrH_2$ is significantly faster under an atmosphere of O_2, suggesting the intermediacy of the acridinyl radical $AcrH^{\bullet}$.

Hydrogen-atom transfer is favored over hydride transfer at roughly the same driving force. This suggests that transfer of an H atom is intrinsically as easy or easier than transfer of a hydride ion. More studies are needed to determine whether this is a general conclusion.

Acknowledgment. We thank Dr. Jasmine R. Bryant for advice on preparing the ruthenium complexes. We are grateful for financial support from the National Institutes of Health (Grant R01-GM50422) to J.M.M. and from the JSPS Research Fellowships for Young Scientists to T.M.

Supporting Information Available: ^{1}H NMR spectra for the oxidations by $\mathbf{Ru^{IV}O^{2+}}$ and for the reaction of $AcrH^+$ with $\mathbf{Ru^{II}OH^+}$, spectral changes and the pseudo-first-order plot for the oxidation of BNAH, and Eyring plots. These materials are available free charge via the Internet at http://pubs.acs.org.

IC048170Q